

Comparing the Corrosion Effects of Two Environments on As-Cast and Extruded Magnesium Alloys

H.J. Martin¹, C. Walton¹, J. Danzy¹, A. Hicks¹, M.F. Horstemeyer¹, P.T. Wang¹

¹Center for Advanced Vehicular Systems (CAVS), Mississippi State University, Box 5405, Mississippi State, MS, USA 39762

Keywords: Magnesium Alloy, Pitting Corrosion, Intergranular Corrosion

Abstract

Magnesium is easily corroded in the presence of saltwater, limiting its use in the automotive industry. The magnesium microstructure greatly affects the corrosion rate, due to various additional elements. In the Center for Advanced Vehicular Systems at Mississippi State University, the effects of immersion and cyclical salt spray testing on various as-cast and extruded magnesium alloys is currently being examined. Previous work on an as-cast AE44 magnesium alloy has demonstrated that individual pit characteristics, such as pit depth, pit area, and pit volume, were deeper and larger following exposure to the immersion environment. However, the data elucidating the corrosion effects on individual pit characteristics has only been seen on as-cast magnesium containing rare earth elements, not on extruded magnesium alloys or zinc-containing magnesium alloys, both common magnesium forms. The research presented here will cover the effects of individual pit characteristics formed on various magnesium alloys due to the different environments.

Introduction

While magnesium is currently used in both the automotive and aerospace industries, its high corrosion rate means that it can only be used in areas that are unexposed to the environment [1-3]. Various elements, such as aluminum, zinc, manganese, and rare earth elements, have been added in an effort to improve the corrosion resistance of magnesium [2, 4-8].

Corrosion resistance has been shown to be highly affected by percentage of aluminum added [2]. The presence of aluminum, in the β -phase precipitate and appearing as $Mg_{17}Al_{12}$, can improve the corrosion resistance of magnesium when the β -phase is continuous [2, 9-11]. However, when the β -phase is small and unconnected, aluminum can lead to the creation of micro-galvanic cells, which reduces corrosion resistance [2, 9-11].

The presence of rare earth elements can also affect the corrosion properties and mechanical properties of magnesium [4-8]. When rare earth elements are present in the β -phase, the creep properties are improved, as well as the corrosion resistance [6-8, 12]. Corrosion resistance is improved due to shift of pitting corrosion, from along the magnesium grain – eutectic boundary to the interior of the magnesium grain [7, 13].

Besides the alloying elements, the presence of an as-cast skin can also affect the corrosion resistance of magnesium. It has been shown on AZ91 that the corrosion of the as-cast skin is 10-fold lower than the bulk AZ91, due to the presence of very small grains [9, 14]. However, extrusion removes the as-cast skin, resulting in a higher corrosion rate.

Pitting corrosion and general corrosion are also affected by the exposure conditions of magnesium. Salt spray testing and

immersion testing are common testing environments, with ASTM standards that were developed separately [15-16]. These two ASTM standards, however, require different concentrations of salt, meaning a direct comparison between the results cannot be made [15-16]. In addition, field corrosion tests do not translate to ASTM standards, leading to an industrial development of cyclical tests [15-18]. Several industrial tests exist, such as Renault ECC1, Volkswagen PV1210, and General Motors GM9540P [18]. These industrial cyclical tests contain a pollution phase and a wet or dry phase in an effort to expose test alloys to environmental conditions that are associated with engine cradles, such as de-icing salt, mud, and condensation [18-19]. However, none of the industrial tests are the same, with varying amounts of NaCl, such as 1%, 5%, and 0.9%, respectively, varying pHs, such as a pH of 4, 6.5-7.2, and 6-9, respectively, and varying exposure times, such as 30 min/day, 4 hrs/day, and 4 x 30 min/day, respectively [18]. In addition, the General Motors tests include other chemicals, such as $CaCl_2$ and $NaHCO_3$ [18]. These differences mean that the results from the multitude of industrial tests cannot be compared [18-19]. In an effort to develop a cyclical test where the results could easily compare with the results from an immersion test, four cyclical test combinations were examined, which showed that a 3.5% NaCl solution which cycled through salt-spray, 100% humidity, and a drying phase proved to be the most corrosive [20]. The goal of this research, then, is to study various magnesium alloys in as-cast or extruded form in order to understand how individual pits grow in depth, surface area, and volume to determine how the various alloying elements affect individual pit characteristics based on environment.

Materials and Methods

Testing

Twelve AZ61 coupons and twelve AM30 coupons (2.54 cm x 2.54 cm x varying thicknesses) were cut from an extruded crash rail provided by Ford using a CNC Mill (Haas, Oxnard, CA). Twelve AZ31 coupons were cut from extruded sheets using a vertical band saw (MSC Industrial Supply Company, Columbus, MS). Twelve AE44 coupons (2.54 cm x 2.54 cm x varying thicknesses) were cut from an as-cast engine cradle provided by Meridian Technologies using a vertical band saw. The coupon surfaces were left untreated to test the corrosion effects on the extruded AZ31 and AZ61 magnesium alloys and on the as-cast AM60 and AE44 magnesium alloys.

Two different test environments were used in this study: salt spray testing and immersion. For salt spray testing, a Q-Fog CCT (Q-Panel Lab Products, Cleveland, OH) was used to cycle through three stages set at equal times, including a 3.5 wt.% NaCl spray at 35°C, 100% humidity using distilled water at 35°C, and a drying purge at 35°C. For immersion testing, an aquarium with an aeration unit was filled with 3.5 wt.% NaCl at room temperature. For both tests, the six coupons per test environment were hung at 20° to the horizontal, as recommended by ASTM B-117 [15]. The

coupons were exposed to the test environment for 1 h, removed, rinsed with distilled water to remove excess salt, and dried. No chemicals were used to clean the surfaces following the corrosion experiments to ensure that the pits and surfaces were unchanged over time. Following the profilometer analysis, the coupons were then placed back into the test environment for an additional 3 h, an additional 8 h, an additional 24 h, and another 24 h. These times allowed for a longitudinal study to follow pit growth and surface changes over time, where $t_0 = 0$, $t_1 = 1$ h, $t_2 = 4$ h, $t_3 = 12$ h, $t_4 = 36$ h, and $t_5 = 60$ h. Between analyses and environmental exposures, the coupons were stored in a desiccator to ensure that no further surface reactions occurred.

Analysis

Following each time exposure, the coupons were analyzed using optical microscopy and laser profilometry. The coupons were weighed prior to testing and following each exposure on two different scales and an average was taken. Four thickness measurements were taken on each sample prior to and following the test. Because the coupons were cut from an engine cradle, the thicknesses of the coupons varied from side to side, meaning an average was taken per coupon based on the four measurements. Measurements for all figures were averaged from the data with error bars based on one standard deviation.

Laser profilometry was used to scan a 1 mm by 1 mm area on two coupons per environment following each test cycle (Talysurf CLI 2000, Taylor Hobson Precision Ltd, Leicester, England). The resulting 2-D and 3-D images were used to document the changes in the pit characteristics due to the different test environments over the six cycles (Tallymap Universal, v. 3.18, Taylor Hobson Precision Ltd, Leicester, England). Data collected was averaged based on fourteen pits within the same 1 mm by 1 mm area, for a total of twenty-eight data points per environment per cycle. The software was used to calculate pit maximum depth, pit mean depth, pit surface area, and pit volume.

Results

Figures 1 and 2 show the average weight and thickness change, respectively, over the five exposure times for the immersion and salt spray surfaces on the various magnesium alloys being compared. As one can see, all surfaces follow similar logarithmic trends for weight change (Figure 1) and thickness change (Figure 2).

Figure 3 shows the maximum pit depth over the five exposure times for the immersion and salt spray surfaces on the various magnesium alloys being compared. As one can see, the salt spray surfaces followed second-order polynomial trends, while the immersion surfaces followed more linear trends. The as-cast AM60 surfaces showed the deepest pits as compared to the other surfaces, while the as-cast AE44 surfaces and extruded AZ61 surfaces showed the shallowest pit formation.

Figure 4 shows mean pit depth over the five exposure times for the immersion and salt spray surfaces on the various magnesium alloys being compared. As with maximum pit depth, most salt spray surfaces followed a second-order polynomial, while most immersion surfaces followed an almost linear trend. However, the trend on the as-cast AM60 surfaces switched, with the salt spray surface following an almost linear trend and the immersion

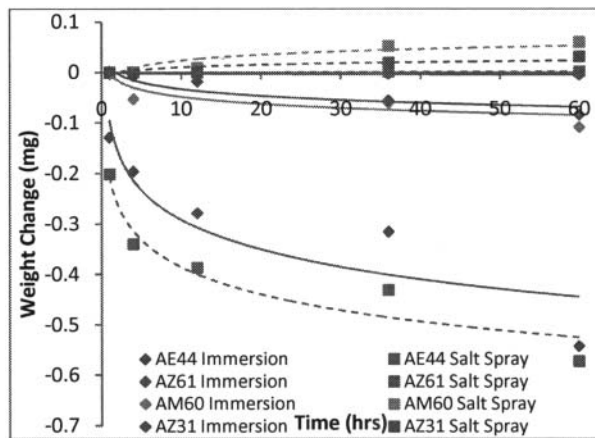


Figure 1: Average weight change of various magnesium alloys based on test environment over 60 h. Notice that all surfaces followed logarithmic trends.

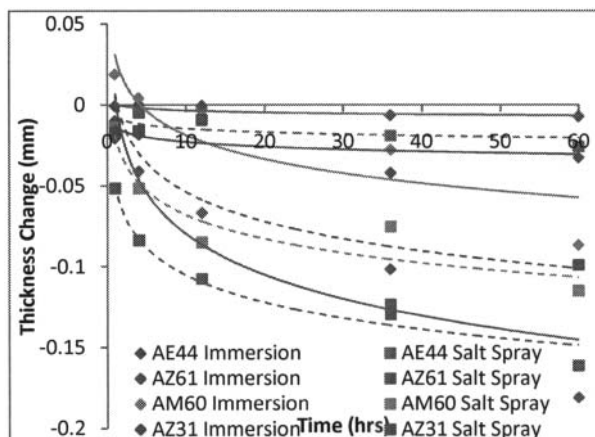


Figure 2: Average thickness change of various magnesium alloys based on test environment over 60 h. Notice that all surfaces followed logarithmic trends.

surface following a second-order polynomial trend. The as-cast AM60 surface still showed the deepest pits, though.

Figure 5 shows the changes in the pit surface area, which is the area calculated over the 3-D area covered by the pit using laser profilometry, over the five exposure times for the immersion and salt spray surfaces on the various magnesium alloys being compared. For all surfaces, the pit surface area followed second-order polynomial trends, with the largest pit surface area occurring on the as-cast AM60 surface and the smallest pit surface area occurring on the as-cast AE44 surface. Notice also that both AM60 surfaces were divided by 10 to bring the values for pit surface area within the range of the other values, in order to follow second-order polynomial trends, while the immersion surfaces appeared to follow more linear trends.

Figure 6 shows the changes in the pit volume over the five exposure times for the immersion and salt spray surfaces on the various magnesium alloys being compared, using laser profilometry. As with the pit surface area, all surfaces followed second-order polynomial trends, with the largest pit volume occurring on the as-cast AM60 surface and the smallest pit surface

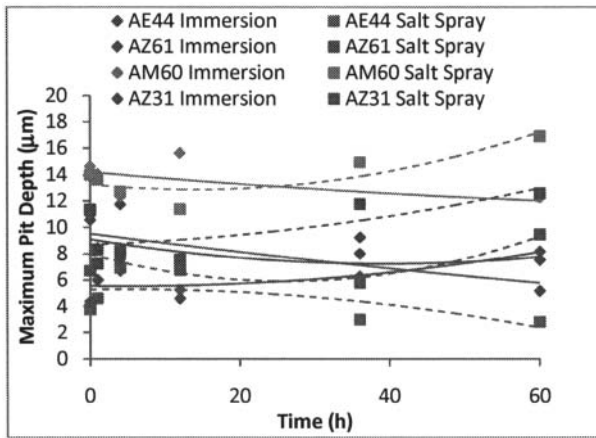


Figure 3: Maximum pit depth of various magnesium alloys based on test environment over 60 h. Notice that all salt spray surfaces exposure times for the immersion and salt spray surfaces on the various magnesium alloys being compared.

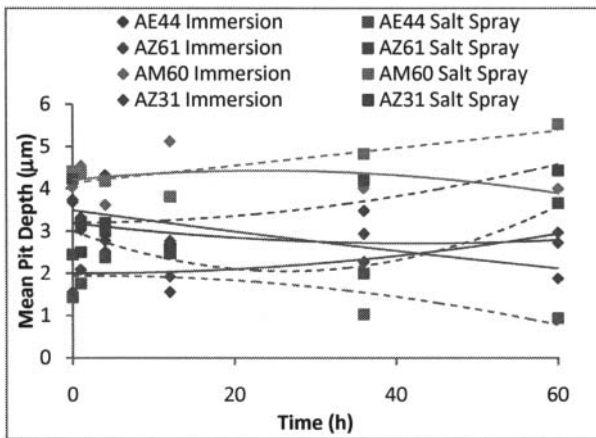


Figure 4: Mean pit depth of various magnesium alloys based on test environment over 60 h. Notice that the salt spray surfaces, except for AM60, followed second-order polynomial trends while the immersion surfaces followed mostly linear trends, again except for AM60.

area occurring on the as-cast AE44 surface. Notice also that both AM60 surfaces were divided by 10 to bring the values for pit volume within the range of the other values, in order to prevent a large y-axis that compressed the other three volume values.

Discussion

More weight loss is seen on the immersion surfaces as compared to the salt spray surfaces, except with respect to the as-cast AE44 surfaces (Figure 1). Because the samples in the salt spray environment are not continuously exposed to water, the water could not react with the surface continuously, meaning that less weight was lost from the surface of the material. However, higher thickness loss was seen on the salt spray surfaces as compared to the immersion surfaces, likely due to changes around the outsides of the coupons exposed to the cyclical salt spray (Figure 2). Since water was not continuously removing debris and salt from the edges in the cyclical salt spray, the debris and salt remained on the

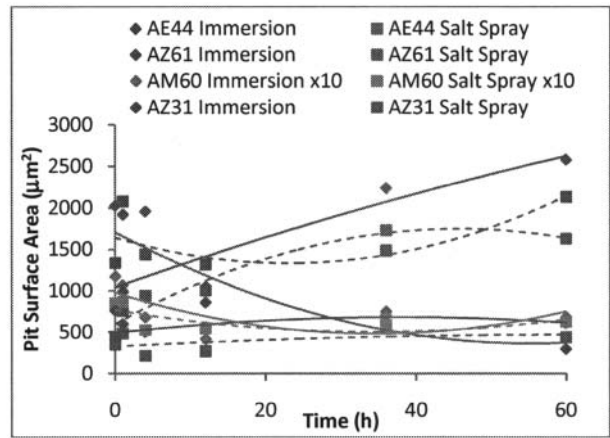


Figure 5: Pit surface area of various magnesium alloys based on test environment over 60 h. Notice that all surfaces followed second-order polynomial trends. Also notice that the as-cast AM60 surfaces had the largest pit surface area, which was divided by 10 to ensure all data could be seen. Notice also that the as-cast AE44 surfaces had the smallest pit surface area.

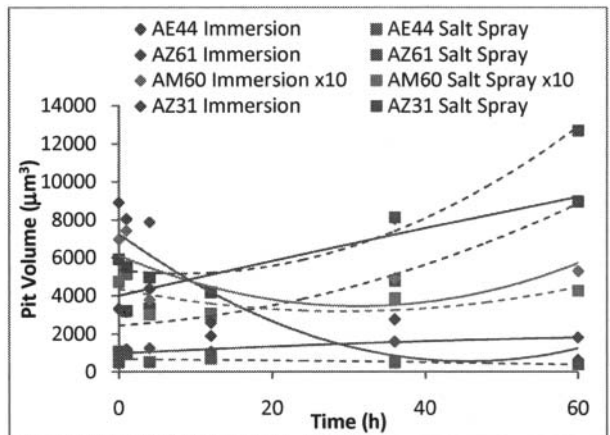


Figure 6: Pit volume of various magnesium alloys based on test environment over 60 h. Notice that all surfaces followed second-order polynomial trends. Also notice that the as-cast AM60 surfaces had the largest pit volume, which was divided by 10 to ensure all data could be seen. Notice also that the as-cast AE44 surfaces had the smallest pit volume.

edges, reacting with and degrading the magnesium. Since weight was measured with a scale, placement on the scale would not affect the weight. However, thickness was measured with calipers, so the placement of the calipers on the outside of each of the coupons would affect the thickness measurements, and the debris degrading the edges would negatively affect the thickness measurements.

Weight loss and thickness loss are not the only measure of corrosion, however. Pitting corrosion is highly detrimental but may not be detected by changes in weight and thickness. Instead, monitoring for pitting characteristics, such as pit depth, pit surface area, and pit volume allow one to determine how the pits grow over time. The maximum pit depth indicates how deep a pit is at its deepest spot, which is useful in determining the long term

effect of that pit on the material or if the pit can cause a breach (Figure 3). The mean pit depth indicates, on average, how deep the pit is, which is useful in seeing how the pit is growing outwards relative to how the pit is growing downwards (Figure 4). The pit surface area is the 3-D area covered by the pit (Figure 5), while the pit volume is the volume of the material removed during the pitting process (Figure 6). Since pits are essentially cones, the 3-D area and volume incorporate the mean pit depth and the maximum pit depth in the calculation of surface area and volume, allowing one to determine how the growth of the pit relates to the depth of the pit. Table I shows the overall rankings based on the charts of the differences in pit characteristics.

Table I: Overall and Group Ranking of Pit Characteristics by Environment

Environment	Alloy	Depth	Sur. Area	Volume
Immersion	AZ31	6 3	3 2	4 2
	AE44	7 4	8 4	7 4
	AZ61	5 2	6 3	6 3
	AM60	3 1	1 1	1 1
Salt Spray	AZ31	2 2	4 2	3 2
	AE44	8 4	7 4	8 4
	AZ61	4 3	5 3	5 3
	AM60	1 1	2 1	2 1

The initial number in each column is the ranking of each line on the graphs based on the final time. The second number in each column is the ranking of each line within the environment based on the final time. Notice that the trend changes for the depth, but stays the same for the pit surface area and pit volume. Also remember that AM60 was divided by 10 on the graphs to ensure that all data could be seen, which is why it is 1 and 2 in this table.

Four different factors affect the pit depth, pit surface area, and pit volume: general corrosion, the form of magnesium (as-cast versus extruded), the corrosive environment, and the type of magnesium alloy. When looking at the effects of general corrosion (Figures 1 and 2), one can see that some magnesium alloys, specifically both environments of AE44 and the immersion environment of AZ61, showing decreasing values in pit depth, while only AE44 shows a decreasing surface area and volume. The decrease, instead of increases, means that general corrosion is acting on the surface faster than the pits can grow. While the pits were initially able to begin corroding the AE44 material, over time, general corrosion stopped pit growth and instead corroded the entire surface equally.

The first factor that can affect the change in pit characteristics, general corrosion, only really affected the as-cast AE44. The other materials could experience differences in pit formation due to the form of corrosion, the environment, or the magnesium alloying elements. When one compares the pit depth based on the form of magnesium, the extruded AZ61 and AZ31 materials fall in the middle of the two as-cast magnesiums (Table I, Figures 3 and 4). In addition, when looking at the surface area and volume, the form of magnesium does not play a significant role in the growth of the pits, with the extruded magnesium alloys again occurring in the middle of the as-cast materials (Please remember that the AM60 material was divided by 10 in order to fit the lines on the graph and ensure all data could be seen) (Table I, Figures 5 and 6). By looking at the individual pit characteristics, averaged over 14 pits per environment per time, one can see that the form of magnesium plays very little role in the formation or growth of individual pits.

Because general corrosion only affected AE44 and the forming of the magnesium alloys did not affect individual pit formation and growth, one of the other two factors, the corrosive environment or the magnesium alloy, must account for the differences in pitting on the four magnesium alloys (Table I, Figures 3-6). When looking at the corrosive environments regardless of alloy, one sees that, with the exception of AZ61, the pits in the immersion environment decreased throughout the experiment time (Table I, Figures 3 and 4). Because pitting corrosion is the initial mechanism of corrosion and general corrosion “catches” up to pitting corrosion, the continuous exposure of water to the magnesium surface allowed the magnesium surrounding the pits to degrade, resulting in less deep pits. However, because the pits in the salt spray environment were not continuously exposed to water, but the chloride ions could become trapped within the pits, the pits were able to grow in depth over time, with the exception of AE44. With respect to pit surface area, there were no overall trends when examining the different environments, as some materials increased throughout the experiment time (AZ31 immersion, AE44 salt spray), one decreased throughout the experiment time (AE44 immersion), and the remaining followed parabolic curves, positively (both AZ61 environments) or negatively (both AM60 environments, AZ31 salt spray) (Figure 5). The pit volume data showed the same lack of trends between the two environments (Figure 6).

The differences in environment can be attributed to the differences in pit characteristics, although the environment alone cannot be responsible for the differences in pit characteristics. If environment was solely responsible for the differences, then one would expect to see that all surfaces followed the same trends, regardless of alloying elements. Either the salt spray environment would produce the largest, deepest pits because of pit debris allowing the autocatalytic nature of pitting to proceed even during the drying phase [1] or the immersion environment would produce the largest, deepest pits because of the continuous presence of chloride ions. Instead, one sees that a difference between environments exists based on alloying elements, where the pit depth for AM60, AZ31, and AZ61 are higher on the salt spray surfaces and the pit depth for AE44 is higher on the immersion surfaces. In addition, the pit surface area is larger on the AZ31, AM60, and AE44 immersion surfaces, while AZ61 has a higher pit surface area on the salt spray surfaces. Lastly, the pit volume on AZ31 and AZ61 is higher on the salt spray surfaces, while the pit volume on AM60 and AE44 is higher on the immersion surfaces.

When it comes to alloying elements, though, one can see a major difference between the four different magnesium alloys (Table I). AM60 had the deepest pits, with the largest pit surface area and largest pit volume, while AE44 had the shallowest pits with the smallest pit surface area and smallest pit volume. The other two alloys, AZ31 and AZ61, showed differences in pit depth, pit surface area, and pit volume, but were within the differences experienced by AE44 and AM60. The differences in pit characteristics must then be related to the alloying elements, although they cannot be attributed to the percentage of aluminum. While it has been shown that up to 10% aluminum can increase corrosion resistance [2], if the percentage of aluminum alone was responsible for the differences in pitting corrosion, then one would expect that AZ31, with 3% aluminum, would be most heavily corroded, followed by AE44 (4% Al), with AZ61 (6% Al) and AM60 (6% Al) tied. As previously stated, though, that is not

the case, as AM60 is the most heavily corroded and AE44 is the least corroded.

While the reason that AE44 is corroded less than the other three materials can be explained, the reason that AM60 is more heavily corroded, even in the as-cast state, at this point cannot be explained. Currently, other AM alloys compositions are being corroded to see if manganese has an influence on the corrosion or if the aluminum-manganese percentage is the cause. AE44 corroded less than either of the AZ alloys due to the way in which AE44 corrodes. It has been shown that on AE44, the pits form within the magnesium grains and not along the intergranular boundaries due to the addition of the rare earth elements [7, 13]. While the pit can begin growing, both in depth and in area/volume, once the pit has corroded the entire grain, there is no further way for that pit to grow. This means that, once the pit has corroded the entire grain, there is nowhere else for the pit to grow, resulting in a pit growth stoppage and preventing a breach through the material.

Conclusions

Four magnesium alloys in two forms, as-cast AE44, as-cast AM60, extruded AZ61, and extruded AZ31, were examined in two corrosive environments, immersion and salt spray. Bulk coupon characteristics, weight loss and thickness loss, as well as individual pitting characteristics, maximum pit depth, mean pit depth, pit surface area, and pit volume, were quantified over 60 hours. With respect to the individual pitting characteristics, the form of magnesium and the environment appeared to have minimal affect on the pit depth, pit surface area, or pit volume, indicating that once the pits began forming, the environment nor the form would affect their growth. However, alloying elements did affect pit growth. AM60 had deeper pits, with the largest pit surface areas and largest pit volumes, while AE44 had the shallowest pits, with the smallest pit surface areas and pit volumes. The extreme corrosion of AM60 cannot yet be explained, while the small corrosion of AE44 is attributed to the corrosion characteristics controlled by the addition of the rare earth elements. Overall, the most heavily corroded magnesium alloy, determined by combining general and pitting corrosion, was AM60, followed by AZ31, AZ61, and AE44, respectively.

References

[1] M.G. Fontana, Corrosion Principles, in: M.G. Fontana (Eds.), *Corrosion Engineering*, McGraw-Hill, Boston, 1986, pp. 12-38.

[2] G. Song, A. Atrens, "Understanding Magnesium Corrosion – A Framework for Improved Alloy Performance", *Advanced Engineering Materials* 5 (2003) 837-858.

[3] BA Shaw, Corrosion Resistance of Magnesium Alloys, in: L.J. Korb, ASM (Eds.), *ASM Handbook*, Vol. 13A: Corrosion, Ninth Ed., ASM International Handbook Committee, Metals Park, 2003, pg. 692.

[4] J.D. Majumdar, R. Galun, B. Mordike, I. Manna, "Effect of laser surface melting on corrosion and wear resistance of a commercial magnesium alloy", *Materials Science and Engineering A*, 361 (2003) 119-129.

[5] C. Blawert, E.D. Morales, W. Dietzel, K.U. Kainer, "Comparison of Corrosion Properties of Squeeze Cast and Thixocast MgZnRE Alloys", *Materials Science Forum*, 488-489 (2005) 697-700.

[6] W. Liu, F. Cao, L. Chang, Z. Zhang, J. Zhang, "Effect of rare earth element Ce and La on corrosion behavior of AM60 magnesium alloy", *Corrosion Science*, 51 (2009) 1334-1343.

[7] W. Liu, F. Cao, L. Zhong, L. Zheng, B. Jia, Z. Zhang, J. Zhang, "Influence of rare earth element Ce and La addition on corrosion behavior of AZ91 magnesium alloy", *Materials and Corrosion*, 60 (2009) 795-803.

[8] Y.L. Song, Y.H. Liu, S.R. Yu, X.Y. Zhu, S.H. Wang, "Effect of neodymium on microstructure and corrosion resistance of AZ91 magnesium alloy", *Journal of Materials Science*, 42 (2007) 4435-4440.

[9] G. Song, "Recent Progress in Corrosion and Protection of Magnesium Alloys", *Advanced Engineering Materials*, 7 (2005) 563-586.

[10] M.C. Zhao, M. Liu, G. Song, A. Atrens, "Influence of pH and chloride ion concentration on the corrosion of Mg alloy ZE41", *Corrosion Science*, 50 (2008) 1939-1953.

[11] G. Song, A. Atrens, X. Wu, B. Zhang, "Corrosion behavior of AZ21, AZ501, and AZ91 in sodium chloride", *Corrosion Science*, 40 (1998) 1769-1791.

[12] Y.L. Song, Y.H. Liu, S.H. Wang, S.R. Yu, X.Y. Zhu, "Effect of cerium addition on microstructure and corrosion resistance of die cast AZ91 magnesium alloy", *Materials and Corrosion*, 58 (2007) 189-192.

[13] N. Birbilis, M.A. Easton, A.D. Sudholz, S.M. Zhu, M.A. Gibson, "On the corrosion of binary magnesium-rare earth alloys", *Corrosion Science*, 51 (2009) 683-689.

[14] G. Song, A. Atrens, M. Dargusch, "Influence of microstructure on the corrosion of diecast AZ91D", *Corrosion Science*, 41 (1998) 249-273.

[15] ASTM B117 - 07a (2007) Standard Practice for Operating Salt Spray (Fog) Apparatus, Vol. 03.02, 2007.

[16] ASTM G31 - 72 (2004) Standard Practice for Laboratory Immersion Corrosion Testing of Metals, Vol. 03.02, 2004.

[17] K.R. Baldwin, C.J.E. Smith, "Accelerated corrosion tests for aerospace materials: current limitations and future trends", *Aircraft Engineering and Aerospace Technology*, 71 (1999) 239-44.

[18] N. LeBozec, N. Blandin, D. Thierry, "Accelerated corrosion tests in the automotive industry: A comparison of the performance towards cosmetic corrosion", *Materials and Corrosion* 59 (2008) 889-94.

- [19] G. Song, D. St.John, C. Bettles, G. Dunlop, "The corrosion performance of magnesium alloy AM-SC1 in automotive engine block applications", *Journal of the Minerals, Metals, and Materials Society*, 57 (2005) 54-6.
- [20] H.J. Martin, M.F. Horstemeyer, P.T. Wang, "Effects of Variations in Salt-Spray Conditions on the Corrosion Mechanisms of an AE44 Magnesium Alloy", *International Journal of Corrosion*, 2010 (2010) 1-10 doi: 10.1155/2010/602342.
- [21] M.F. Horstemeyer, J. Lathrop, A.M. Gokhale, M. Dighe, "Modeling stress state dependent damage evolution in a cast Al-Si-Mg aluminum alloy", *Theoretical and Applied Fracture Mechanics*, 33 (2000) 31-47.